# Quantum search algorithms on a regular lattice

Birgit Hein[1,2] and Gregor Tanner[1]

[1]*School of Mathematical Sciences, University of Nottingham, University Park, Nottingham NG7 2RD, United Kingdom*
[2]*Institute for Theoretical Physics, University of Regensburg, 93040 Regensburg, Germany*

Quantum algorithms for searching for one or more marked items on a $d$-dimensional lattice provide an extension of Grover's search algorithm including a spatial component. We demonstrate that these lattice search algorithms can be viewed in terms of the level dynamics near an avoided crossing of a one-parameter family of quantum random walks. We give approximations for both the level splitting at the avoided crossing and the effectively two-dimensional subspace of the full Hilbert space spanning the level crossing. This makes it possible to give the leading order behavior for the search time and the localization probability in the limit of large lattice size including the leading order coefficients. For $d = 2$ and $d = 3$, these coefficients are calculated explicitly. Closed form expressions are given for higher dimensions.

## I. INTRODUCTION

Quantum random walks as introduced by Aharonov *et al.* [1] in 1993 have gained considerable attention over the last decade or so. It could be demonstrated that a quantum version of a classical random walk has transport properties which exhibit polynomial or even exponential speed-up compared to a classical random walk; see [2–4] for overviews. This has recently led to increased efforts for implementing quantum random walks experimentally. In particular, one-dimensional quantum walks have been realized using neutral atoms in optical lattices [5], with trapped ions [6–8], and using coupled optical wave guides [9] and single photons [10].

One of the most fascinating applications based on quantum random walk concepts is the spatial quantum search algorithm. Like Grover's search algorithm [11,12] for searching an unstructured data base, quantum walk search algorithms can (usually) achieve a quadratic speed-up compared to the corresponding classical search. The most prominent algorithms are the search on a hypercube introduced by Shenvi *et al.* [13] and the search on a $d$-dimensional lattice presented by Childs and Goldstone [14] in a continuous time version and by Ambainis, Kempe, and Rivosh (AKR) [15] as a discrete time algorithm. In particular, it has been pointed out that the search in a two-dimensional lattice is critical with the number of search steps scaling like $O(\sqrt{N}\log N)$ whereas quantum search algorithms on the hypercube as well as for lattices of dimension $d \geqslant 3$ scale like $O(\sqrt{N})$; here, $N$ is the number of vertices. Expressions for the leading order coefficients for the search time in the hypercube have been given in [16]; proposals for improving the efficiency of the hypercube search can be found in [17]. In [18], it has been shown that the number of steps for solving the search problem on a two-dimensional lattice can be decreased to $O(\sqrt{N\log N})$ by modifying the quantum walk search algorithm, thus coming closer to the theoretical lower bound $\Omega(\sqrt{N})$ [19].[1] By changing the starting state, it has been demonstrated in [20] that quantum search algorithms

on lattices can also be used in a sender-receiver configuration. Remarkably, this makes it possible to communicate across the lattice by sending information exclusively between two (or more) marked vertices where neither the sender nor the receivers need to know each other's position.

We will in the following focus on the AKR search algorithm on $d$-dimensional lattices. Extending the ideas and techniques from [16], we will give improved estimates for the approximate eigenstate of the walk localized on the target vertex. This makes it possible to give closed form expressions for the leading order coefficients for both the search time and the search efficiency, that is, the overlap of the localized state with the target vertex. The paper is structured as follows. The search algorithm on the lattice and the basic vectors spanning the search space in the full Hilbert space are introduced in Sec. II; this is followed by a detailed calculation of the normalization constant for the approximate eigenvector localized on the target vertex in Sec. III. In Sec. IV, we analyze the spectral gap at the avoided crossing in an (approximately) invariant two-dimensional subspace. The results for leading order contributions to the localization time and the amplitude at the target vertex are given in Sec. V.

## II. A QUANTUM SEARCH ON A $d$-DIMENSIONAL SQUARE LATTICE: INTRODUCING THE ALGORITHM

Quantum search algorithms—like Grover's search—are usually described in terms of two unitary matrices: a quantum or wave propagator acting uniformly on the search space and a "marker" (or oracle) matrix which deviates from the identity only locally near the marked item. We will discuss here a lattice search algorithm of this type which was first introduced in [15]. We will limit the discussion to the search of one target vertex only. A generalization to more than one marked item is straightforward and is discussed in [15,20]. We will first introduce the propagator without a marked vertex leading to a quantum random walk on the lattice. The full quantum search

---

[1]The scaling behavior of a function will be denoted as follows: $f(x) = O(g(x))$ indicates that there exist two positive constants $x_0 > 0$ and $a > 0$, such that for all $x > x_0$ the inequality $0 \leqslant f(x) \leqslant ag(x)$ is true. Similarly, $f(x) = \Omega(g(x))$ will be written

if $0 \leqslant bg(x) \leqslant f(x)$ for all $x > x_0$ for some constants $x_0$, $b > 0$. Furthermore, $f(x) = \Theta(g(x))$ denotes that $f(x) = O(g(x))$ as well as $f(x) = \Omega(g(x))$.

algorithm and an analysis of the search mechanism will be given in Sec. II B.

### A. A quantum random walk on a $d$-dimensional lattice

We consider a $d$-dimensional regular lattice with $n$ vertices along each dimension, that is, $N = n^d$ vertices overall. The positions of the vertices in the lattice are defined by the set of vectors $|x\rangle = \vec{x} = (x_1, x_2, \ldots, x_d)$ with integer coordinates $x_i \in \{0, 1, \ldots, n-1\}$. Periodic boundary conditions will be assumed throughout.

Following the spirit of quantum graph theory, we consider quantum waves propagating freely along one-dimensional bonds connecting adjacent vertices [21,22]. Waves undergo scattering at the vertices described by a $2d \times 2d$ scattering matrix $\sigma$, where $2d$ is the number of bonds connected at each vertex. The scattering mechanism is the same at all vertices and the quantum dynamics on the lattice is in fact equivalent to a quantum random walk; see [23]. [The unitary scattering matrix $\sigma$ can then also be interpreted as a "coin flip" matrix acting on an internal (spin) degree of freedom of a quantum walker.] The total Hilbert space $\mathcal{H}$ of the problem is described as the tensor product of a vertex or position space $|x\rangle$ and a direction or coin space $|i^{\pm}\rangle$ representing waves traveling in the negative or positive direction along the $i$th axis, $i = 1, \ldots, d$. The dimension of $\mathcal{H}$ is thus $2dn^d = 2dN$.

We chose a scattering matrix $\sigma$ which is unbiased with respect to the outgoing directions (except possibly for back-scattering). A natural choice is Grover's matrix [12] (which incidentally also features prominently in a quantum graph approach using Kirchhoff boundary conditions on the vertices; see [21,22]). That is, we define [15]

$$\sigma = 2|s\rangle\langle s| - \mathbb{1}_{2d}, \tag{1}$$

where $|s\rangle$ is the uniform distribution in coin space, that is,

$$|s\rangle = \frac{1}{\sqrt{2d}} \sum_{i=1}^{d} (|i^+\rangle + |i^-\rangle). $$

We have identical scattering processes at all vertices and we thus define a global coin flip matrix,

$$C = \sigma \otimes \mathbb{1}_N. \tag{2}$$

The wave propagation on the lattice is now given by a "shift" matrix $S$. Waves emanating from vertex $|x\rangle$ in the $i^{\pm}$th direction will reach vertex $|x \pm e_i\rangle$ with $|e_i\rangle$, the unit vector in the $i^+$th direction. Writing $|i^{\pm}x\rangle = |i^{\pm}\rangle \otimes |x\rangle$, we find for the shift matrix $S$,

$$S = \sum_{\vec{x}} \sum_{i=1}^{d} (|i^+ x - e_i\rangle\langle i^- x| + |i^- x + e_i\rangle\langle i^+ x|). \tag{3}$$

This is a natural choice for a moving shift since a walker leaving vertex $\vec{x}$ in direction $i^+$, enters vertex $\vec{x} + \vec{e}_i$ from direction $i^-$.

The quantum random walk $U_0$ is defined by first applying the global coin flip and then the moving shift,

$$U_0 = SC. \tag{4}$$

In what follows, the eigenvectors and eigenvalues of $U_0$ will be of importance; these have been discussed in some detail in [15]. Using the tensor product, we write each eigenvector of $U_0$ as a vector in coin space $|u_{\vec{k}}^c\rangle$ and a position space vector $|X_{\vec{k}}\rangle$ according to

$$\left| \phi_{\vec{k}}^c \right\rangle = \left| u_{\vec{k}}^c \right\rangle \otimes |X_{\vec{k}}\rangle,$$

where $\vec{k}$ is a $d$-dimensional vector with components $k_i \in \{0, 1, \ldots, n-1\}$ and $c = 1, \ldots, 2d$. The vector in position space can be factorized in the form $|X_{\vec{k}}\rangle = \bigotimes_{i=1}^{d} |\chi_{k_i}\rangle$, where the $|\chi_{k_i}\rangle$ are obtained from the canonical basis vectors of position space using a Fourier transformation, that is,

$$\left| \chi_{k_i} \right\rangle = \frac{1}{\sqrt{n}} \sum_{j=0}^{n-1} \alpha^{k_i j} |j\rangle \quad \text{where} \quad \alpha = e^{2\pi i/n}. \tag{5}$$

The thus obtained basis provides a convenient way to denote the eigenvectors in position space.

For the quantum search, only $2N - 1$ of the $2dN$ eigenvectors of $U_0$ are important, namely, those having a coin space component not orthogonal to $|s\rangle$. These vectors are the one-eigenvector $|\phi_0\rangle = |s\rangle \otimes |X_{\vec{0}}\rangle$, which is the uniform distribution, and two eigenvectors [15]

$$|\phi_{\vec{k}}^{\pm}\rangle = |u_{\vec{k}}^{\pm}\rangle \otimes |X_{\vec{k}}\rangle \tag{6}$$

for each $\vec{k} \neq \vec{0}$ with complex conjugated eigenvalues $e^{\pm i\theta_{\vec{k}}}$, and

$$\cos\theta_{\vec{k}} = \frac{1}{d} \sum_{i=1}^{d} \cos\frac{2\pi k_i}{n}.$$

The expressions for the vector $|u_{\vec{k}}^{\pm}\rangle$ in coin space become more and more cumbersome with increasing $d$ and we will not attempt to give closed form expressions here. However, it has been shown in [15] that

$$\langle s | u_{\vec{k}}^{\pm}\rangle = \frac{1}{\sqrt{2}}, \tag{7}$$

which is all we need in what follows. In addition, one has $(d-1)N + 1$ eigenvectors with eigenvalue 1 and $(d-1)N$ eigenvectors with eigenvalue $-1$ all with coin components perpendicular to $|s\rangle$. Note that the high degeneracies in the $\pm 1$ eigenspaces are due to the special choice of the coin flip matrices $\sigma$ and thus $C$.

### B. The quantum search algorithm

#### 1. The quantum search matrix

We now assume that the lattice contains one marked vertex at (a yet unknown) position $\vec{v}$; here, the marking is done by applying a different coin flip or scattering matrix $\sigma'$ at this target vertex $|v\rangle$. The search algorithm is then defined as

$$U_1 = SC', \tag{8}$$

$$C' = C - (\sigma - \sigma') \otimes |v\rangle\langle v|. \tag{9}$$

Note that, since $|v\rangle\langle v|$ is a projection on the target vertex, the additional term changes at most $4d^2$ matrix elements in $U_0$. As $U_0$ is a $2dN \times 2dN$ matrix, $U_1$ is identical to $U_0$ up to a local perturbation and the quantum search algorithm can be regarded as a locally perturbed quantum random walk.
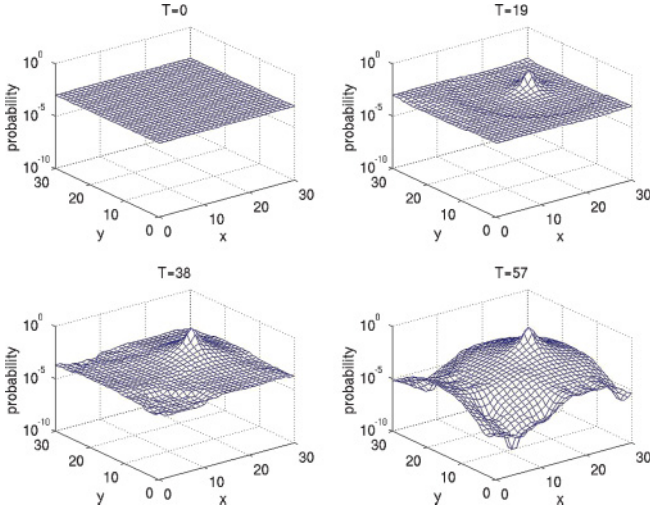
FIG. 1. (Color online) Probability distribution of the quantum walk on a $31 \times 31$ lattice for a number of time steps $t$ (on a logarithmic scale).

Following AKR we define $\sigma' = -\mathbb{1}_{2d}$ which leads after some algebra to

$$U_1 = U_0(1 - 2|sv\rangle\langle sv|). \qquad (10)$$

The perturbed quantum walk is shown in Fig. 1; starting from the uniformly distributed state $|\phi_0\rangle$ and applying $U_1$ for $t$ time steps with $t = 0, 19, 38$, and 57, one observes a localization on the target vertex. Plotted here is the probability (wave amplitude squared) on a logarithmic scale.

Following the analysis developed for the hypercube in [16], we now define a one-parameter family of unitary matrices $U_\lambda$ for the $d$-dimensional lattice:

$$U_\lambda = U_0 + (e^{i\pi\lambda} - 1)U_0|sv\rangle\langle sv|. \qquad (11)$$

This makes it possible to extrapolate smoothly from the unperturbed walk ($\lambda = 0$) to the AKR search algorithm ($\lambda = 1$) and will be helpful for analyzing the eigenvalues and eigenvectors of $U_\lambda$ near $\lambda = 1$ in terms of the eigenbasis of the unperturbed quantum walk.

Before doing so, we simplify the problem by reducing the size of the Hilbert space. We note that eigenvectors of $U_0$ with eigenvalues $\pm 1$ (except the important vector $|\phi_0\rangle$) are orthogonal to $|sv\rangle$ and thus remain eigenvectors of $U_\lambda$ independent of the value of $\lambda$; this part of $\mathcal{H}$ is thus irrelevant for the localization effect. We define a reduced space $\mathcal{H}'$ by projecting out all $\pm 1$ eigenvectors of $U$ except $|\phi_0\rangle$. This subspace is a $(2N - 1)$-dimensional Hilbert space spanned by $|\phi_0\rangle$ and $|\phi_{\vec{k}}^{\pm}\rangle$ for $\vec{k} \neq \vec{0}$.

The scalar product $\langle\phi_{\vec{k}}^{\pm}|sv\rangle$ can be obtained using (7); thus an expansion of $|sv\rangle$ in terms of eigenvectors of $U_0$ in the reduced space gives

$$|sv\rangle = \frac{1}{\sqrt{N}}|\phi_0\rangle + \frac{1}{\sqrt{2N}}\sum_{\vec{k}\neq\vec{0}}\alpha^{-\vec{k}\vec{v}}(|\phi_{\vec{k}}^{+}\rangle + |\phi_{\vec{k}}^{-}\rangle). \qquad (12)$$

Since $|sv\rangle$ is orthogonal to all eigenvectors of $U_0$ not contained in $\mathcal{H}'$, this expansion also holds for the nonreduced space.
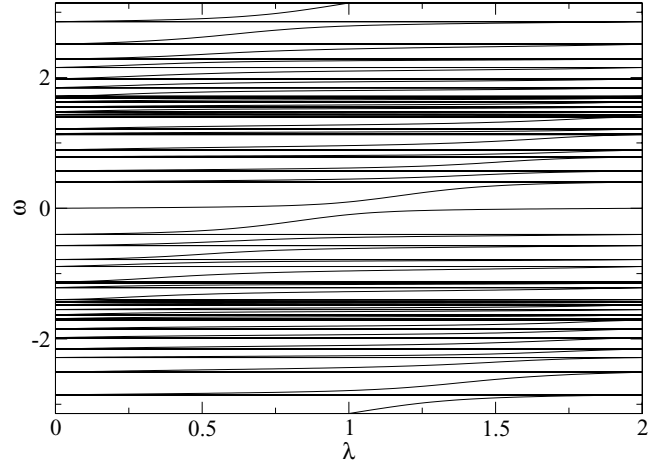


FIG. 2. The eigenphases as functions of $\lambda$ for $n = 11$, $d = 2$.

### 2. Approximate eigenvectors of $U_\lambda$

In the following we will analyze the search algorithm in detail. Our approach is based on the work in [16] and makes it possible to go beyond the results found in [15] by giving explicit leading order coefficients for the search time.

The overall strategy is best explained by considering briefly the spectrum of eigenphases $\{\omega_i\}$ of $U_\lambda$; in Fig. 2, the eigenphases are shown for an $11 \times 11$ lattice in the reduced space $\mathcal{H}'$. The local perturbation leads to a set of avoided crossings in the spectrum, most notably at $\lambda = 1$, $\omega = 0$. This avoided crossing is formed by the state $|\phi_0\rangle$ (which is a 1 eigenstate of U) and "another" state, which we will denote $|v_\lambda\rangle$ in what follows. It will be argued that $|v_\lambda\rangle$ is localized in the vicinity of the target vertex and that the subspace $\{|\phi_0\rangle, |v_\lambda\rangle\}$ is an approximate basis for the two-dimensional eigenspace spanned by the exact eigenstates at the crossing. The quantum search amounts then to a rotation in this two-dimensional subspace of $\mathcal{H}'$ similar to the mechanism found in Grover's original search. It is important to note that unlike for Grover's algorithm, for the lattice search only approximate expressions for the state $|v_{\lambda=1}\rangle$ are known which will be given below; furthermore, the starting state $|\phi_0\rangle$ has a small overlap with the rest of the spectrum at $\lambda = 1$ leading to losses.

We start by considering the uniform distribution $|\phi_0\rangle$ which is the remaining 1 eigenvector of $U_0$ in $\mathcal{H}'$. One obtains

$$U_\lambda|\phi_0\rangle = |\phi_0\rangle + (e^{i\lambda\pi} - 1)U_0|sv\rangle\frac{1}{\sqrt{N}}, \qquad (13)$$

that is, $|\phi_0\rangle$ is an approximate eigenvector of $U_\lambda$ of order $O(N^{-1/2})$. The remaining components, $U_0|sv\rangle$, are localized on the $2d$ sites next to the target vertex. This can be seen from the definition of the shift operator $S$ in Eq. (3).

To obtain $|v_\lambda\rangle$, we start by expanding the vector in the basis of the unperturbed walk $U_0$, that is,

$$|v_\lambda\rangle = a_0|\phi_0\rangle + \sum_{\vec{k}\neq\vec{0}}(a_{\vec{k}}^{+}|\phi_{\vec{k}}^{+}\rangle + a_{\vec{k}}^{-}|\phi_{\vec{k}}^{-}\rangle), \qquad (14)$$

with a yet unknown set of coefficients $\{a_0, a_{\vec{k}}^{\pm}\}$. Normalization requires

$$|a_0|^2 + \sum_{\vec{k} \neq \vec{0}} (|a_{\vec{k}}^+|^2 + |a_{\vec{k}}^-|^2) = 1. \tag{15}$$

We now make the ansatz

$$U_\lambda |v_\lambda\rangle \approx e^{ig(\lambda)} |v_\lambda\rangle, \tag{16}$$

that is, we assume an approximate eigenvalue equation with a yet unknown eigenvalue $e^{ig(\lambda)}$. This gives rise to a linear system of equations for the $2N - 1$ unknown coefficients $\{a_0, a_{\vec{k}}^{\pm}\}$. We are looking for a second approximate eigenvector which spans the space at the avoided crossing together with $|\phi_0\rangle$, that is, we demand that $|v_\lambda\rangle$ and $|\phi_0\rangle$ are orthogonal which leads to $a_0 = 0$.

A straightforward application of $U_\lambda$ on $|v_\lambda\rangle$ results in

$$U_\lambda |v_\lambda\rangle = \sum_{\vec{k} \neq \vec{0}} (a_{\vec{k}}^+ e^{i\theta_{\vec{k}}} |\phi_{\vec{k}}^+\rangle + a_{\vec{k}}^- e^{-i\theta_{\vec{k}}} |\phi_{\vec{k}}^-\rangle) + (e^{i\pi\lambda} - 1)$$

$$\times \Bigg[ \frac{1}{\sqrt{N}} |\phi_0\rangle + \frac{1}{\sqrt{2N}} \sum_{\vec{k} \neq \vec{0}} \alpha^{-\vec{k}\vec{v}} (e^{i\theta_{\vec{k}}} |\phi_{\vec{k}}^+\rangle$$

$$+ e^{-i\theta_{\vec{k}}} |\phi_{\vec{k}}^-\rangle) \Bigg] \langle sv | v_\lambda \rangle, \tag{17}$$

with $\vec{v}$, the position of the target vertex. In what follows, we set

$$b := \langle sv | v_\lambda \rangle, \tag{18}$$

and define the overall phase factor of $|v_\lambda\rangle$ such that $b$ is real with $0 \leqslant b \leqslant 1$. Note that $b$ determines the overlap of the approximate eigenvector with the target vertex. We will show in the next section that $b$ is of order $O(1/\sqrt{\ln N})$ for $d = 2$ and $O(1)$ for $d \geqslant 3$ at $\lambda = 1$; thus $|v_1\rangle$ is indeed localized at the target vertex.

We now add and subtract the right-hand side of Eq. (16) in (17) and obtain

$$U_\lambda |v_\lambda\rangle$$

$$= e^{ig(\lambda)} |v_\lambda\rangle + \frac{b(e^{i\pi\lambda} - 1)}{\sqrt{N}} |\phi_0\rangle$$

$$+ \sum_{\vec{k} \neq \vec{0}} \Bigg\{ \Bigg[ a_{\vec{k}}^+ (e^{i\theta_{\vec{k}}} - e^{ig(\lambda)}) + \frac{b(e^{i\pi\lambda} - 1)\alpha^{-\vec{k}\vec{v}} e^{i\theta_{\vec{k}}}}{\sqrt{2N}} \Bigg] |\phi_{\vec{k}}^+\rangle$$

$$+ \Bigg[ a_{\vec{k}}^- (e^{-i\theta_{\vec{k}}} - e^{ig(\lambda)}) + \frac{b(e^{i\pi\lambda} - 1)\alpha^{-\vec{k}\vec{v}} e^{-i\theta_{\vec{k}}}}{\sqrt{2N}} \Bigg] |\phi_{\vec{k}}^-\rangle \Bigg\}. \tag{19}$$

An approximate solution is obtained if each of the coefficients in front of the components $|\phi_{\vec{k}}^{\pm}\rangle$ is zero, that is,

$$a_{\vec{k}}^{\pm} = \frac{b(e^{i\pi\lambda} - 1)\alpha^{-\vec{k}\vec{v}} e^{\pm i\theta_{\vec{k}}}}{\sqrt{2N}(e^{ig(\lambda)} - e^{\pm i\theta_{\vec{k}}})}. \tag{20}$$

The resulting vector $U_\lambda |v_\lambda\rangle$ has a component in the $|\phi_0\rangle$ direction of order $O(1/\sqrt{N})$; thus, similar to Eq. (13), $|v_\lambda\rangle$ remains in a subspace spanned by itself and $|\phi_0\rangle$.

The coefficients $a_{\vec{k}}^{\pm}$ enter Eq. (20) also through $b$, that is, (20) represents a set of linear, coupled equations. Assuming $b \neq 0$, Eq. (18) can be divided by $b$ and the system of equations has a solution if and only if

$$1 = \frac{(e^{i\pi\lambda} - 1)}{2N} \sum_{\vec{k} \neq \vec{0}} \left( \frac{e^{i\theta_{\vec{k}}}}{e^{ig(\lambda)} - e^{i\theta_{\vec{k}}}} + \frac{e^{-i\theta_{\vec{k}}}}{e^{ig(\lambda)} - e^{-i\theta_{\vec{k}}}} \right). \tag{21}$$

The avoided crossing occurs at $\lambda = 1$ and $e^{ig(1)} = 1$, for which the right-hand side of Eq. (21) can be obtained directly:

$$\frac{-2}{2N} \sum_{\vec{k} \neq \vec{0}} (-1) = \frac{1}{N} (N - 1) = 1 - \frac{1}{N}, \tag{22}$$

that is, no solution exists which maps a vector $|v_1\rangle$ exactly onto itself and $|\phi_0\rangle$. The error term $1/N$ is small compared to typical coupling terms between basis states $|\phi_{\vec{k}}^{\pm}\rangle$ (which are of the order $1/\sqrt{N}$) and the set of coefficients from Eq. (20) thus define an approximate solution of the eigenvalue Eq. (16). That is, the vector,[2]

$$|v_\lambda\rangle = \frac{b(e^{i\pi\lambda} - 1)}{\sqrt{2N}} \sum_{\vec{k} \neq \vec{0}} \alpha^{-\vec{k}\vec{v}}$$

$$\times \left( \frac{e^{i\theta_{\vec{k}}}}{e^{ig(\lambda)} - e^{i\theta_{\vec{k}}}} |\phi_{\vec{k}}^+\rangle + \frac{e^{-i\theta_{\vec{k}}}}{e^{ig(\lambda)} - e^{-i\theta_{\vec{k}}}} |\phi_{\vec{k}}^-\rangle \right), \tag{23}$$

fulfills to leading order the equation

$$U_\lambda |v_\lambda\rangle = e^{ig(\lambda)} |v_\lambda\rangle + \frac{b(e^{i\pi\lambda} - 1)}{\sqrt{N}} |\phi_0\rangle, \tag{24}$$

where $g(\lambda)$ is defined implicitly by minimizing the expression (21). An expansion of $g(\lambda)$ around $\lambda = 1$ can be obtained successively; see [16]. We will restrict our attention here to the case $\lambda = 1$ and thus $|v_{\lambda=1}\rangle$ for which $g(1) = 0$.

The only unknown quantity in determining $|v_1\rangle$ is the constant $b$ which has dropped out of the equations. Since the vector $|v_1\rangle$ needs to be normalized, $b$ turns out to be a normalization constant.

### III. NORMALIZATION OF $|v_1\rangle$

Evaluating the normalization constant $b$ turns out to be the most laborious and technical part of the derivation. Readers more interested in the final results may want to proceed directly to the result in Eq. (54).

We will in the following restrict ourselves to the case $\lambda = 1$ and thus $e^{ig(1)} = 1$ only. Demanding the vector in Eq. (23) to

---

[2]This vector $|v_{\lambda=1}\rangle$ plays essentially the same role as the vector $|\omega_{\text{good}}\rangle$ considered by AKR [15]. Both vectors are in good approximation in the subspace spanned by the two exact eigenvectors at the crossing. However, the vector in [15] is not orthogonal to $|\phi_0\rangle$ and one needs information about the exact eigenphases of $U_{\lambda=1}$ at the crossing. For the vector presented here, a diagonalization of $U_{\lambda=1}$ is not necessary.

be normalized, one obtains

$$\frac{1}{|b|^2} = \frac{4}{2N} \sum_{\vec{k} \neq \vec{0}} \frac{2}{|1 - e^{i\theta_{\vec{k}}}|^2} \tag{25}$$

$$= \frac{2d}{N} \sum_{\vec{k} \neq \vec{0}} \frac{1}{d - \sum_{i=1}^{d} \cos \frac{2\pi k_i}{n}}, \tag{26}$$

where the sum is taken over all vectors $\vec{k} \neq \vec{0}$ in a $d$-dimensional cube with $k_i \in \{0, 1, \ldots, n-1\}$.

We start by rearranging the total sum into a summation over lower-dimensional objects where only a limited number of entries of $\vec{k}$ are different from 0. That is, we consider the summation over all one-dimensional edges, two-dimensional faces, three-dimensional cubes, and so on, where the nonzero entries $k_i$ vary from 1 to $n - 1$. The edges are obtained by choosing $d - 1$ entries of $\vec{k}$ equal 0, the faces have $d - 2$ entries of $\vec{k}$ equal 0 and higher dimensions accordingly. This new arrangement results in

$$\frac{1}{|b|^2} = \frac{2d}{N} \sum_{\vec{k} \neq \vec{0}} \frac{1}{d - \sum_{i=1}^{d} \cos \frac{2\pi k_i}{n}} \tag{27}$$

$$= \frac{2d}{N} \underbrace{d}_{\substack{\text{number of edges}}} \underbrace{\sum_{j_1=1}^{n-1} \frac{1}{1 - \sum_{l=1}^{1} \cos \frac{2\pi j_l}{n}}}_{\text{contribution of one edge}}$$

$$+ \frac{2d}{N} \underbrace{\binom{d}{2}}_{\substack{\text{number of faces}}} \underbrace{\sum_{j_1, j_2=1}^{n-1} \frac{1}{2 - \sum_{l=1}^{2} \cos \frac{2\pi j_l}{n}}}_{\text{contribution of one face}}$$

$$+ \cdots \tag{28}$$

$$= \frac{2d}{N} \sum_{i=1}^{d} \binom{d}{i} \sum_{j_1, j_2, \ldots, j_i=1}^{n-1} \frac{1}{i - \sum_{l=1}^{i} \cos \frac{2\pi j_l}{n}} \tag{29}$$

$$= \frac{2d}{N} \sum_{i=1}^{d} \binom{d}{i} \left(\frac{n}{\pi}\right)^i I_i, \tag{30}$$

where $I_i$ has been implicitly defined in (30). Using the identity $1 - \cos x = 2 \sin^2 \frac{x}{2}$, we can simplify the sums and obtain

$$I_i = \frac{1}{2} \left(\frac{\pi}{n}\right)^i \sum_{j_1, \ldots, j_i=1}^{n-1} \left(\sum_{l=1}^{i} \sin^2 \frac{\pi j_l}{n}\right)^{-1}. \tag{31}$$

Using Poisson's summation formula, one arrives at

$$I_i = \frac{1}{2} \left(\frac{\pi}{n}\right)^i \int_{\frac{1}{2}}^{n-\frac{1}{2}} dx_1 \sum_{m_1=-\infty}^{\infty} e^{2\pi i m_1 x_1} \ldots$$

$$\int_{\frac{1}{2}}^{n-\frac{1}{2}} dx_i \sum_{m_i=-\infty}^{\infty} e^{2\pi i m_i x_i} \left(\sum_{l=1}^{i} \sin^2 \frac{\pi x_l}{n}\right)^{-1} \tag{32}$$

$$= \frac{1}{2} \int_{\frac{\pi}{2n}}^{\pi - \frac{\pi}{2n}} dy_1 \ldots \int_{\frac{\pi}{2n}}^{\pi - \frac{\pi}{2n}} dy_i,$$

$$\sum_{m_1=-\infty}^{\infty} \cdots \sum_{m_i=-\infty}^{\infty} \frac{e^{2in(m_1 y_1 + \cdots + m_i y_i)}}{\sum_{l=1}^{i} \sin^2 y_l}, \tag{33}$$

where the last equality is due to a reordering of terms and substituting $y_j = \frac{\pi}{n} x_j$ in all integrals.

The dominant contributions come from the terms $m_j = 0$ for all $j = 1, \ldots i$, that is, we write to leading order in the large $n$ limit,

$$I_i = \frac{1}{2} \int_{\frac{\pi}{2n}}^{\pi - \frac{\pi}{2n}} dy_1 \ldots \int_{\frac{\pi}{2n}}^{\pi - \frac{\pi}{2n}} dy_i \frac{1}{\sum_{l=1}^{i} \sin^2 y_l}. \tag{34}$$

Using the symmetry of the sine squared function, the integrals (34) can be simplified to

$$I_i = 2^{i-1} \int_{\frac{\pi}{2n}}^{\frac{\pi}{2}} dy_1 \ldots \int_{\frac{\pi}{2n}}^{\frac{\pi}{2}} dy_i \frac{1}{\sum_{l=1}^{i} \sin^2 y_l}. \tag{35}$$

We are only interested in leading order contributions and will thus use the integral (35) as an approximation for the full set of sums in Eq. (33). The expression (35) will form the starting point of our calculation of the leading order behavior of $|b|$.

### A. Integration of $I_1$

The first integration can be done explicitly and one obtains

$$I_1 = \int_{\frac{\pi}{2n}}^{\frac{\pi}{2}} dy \frac{1}{\sin^2 y} = \cot \frac{\pi}{2n} = \frac{2n}{\pi} + O\left(\frac{1}{n}\right). \tag{36}$$

### B. Integration of $I_2$

To obtain a leading order estimate for

$$I_2 = 2 \int_{\frac{\pi}{2n}}^{\frac{\pi}{2}} dx \int_{\frac{\pi}{2n}}^{\frac{\pi}{2}} dy \frac{1}{\sin^2 x + \sin^2 y}, \tag{37}$$

we first note that the integrand is symmetric with respect to exchanging $x$ and $y$ and, therefore,

$$I_2 = 4 \int_{\frac{\pi}{2n}}^{\frac{\pi}{2}} dx \int_{x}^{\frac{\pi}{2}} dy \frac{1}{\sin^2 x + \sin^2 y}. \tag{38}$$

Now, the $y$ integration is solved by observing that

$$\frac{d}{dx} \frac{\arctan\left(\frac{\tan y}{\tan x} \sqrt{2 \tan^2 x + 1}\right)}{\sin x \sqrt{\sin^2 x + 1}} = \frac{1}{\sin^2 x + \sin^2 y}. \tag{39}$$

Thus,

$$I_2 = 4 \int_{\frac{\pi}{2n}}^{\frac{\pi}{2}} dx \left[ \frac{\arctan\left(\frac{\tan y}{\tan x} \sqrt{2 \tan^2 x + 1}\right)}{\sin x \sqrt{\sin^2 x + 1}} \right]_{y=x}^{\frac{\pi}{2}} \tag{40}$$

$$= 4 \int_{\frac{\pi}{2n}}^{\frac{\pi}{2}} dx \frac{\frac{\pi}{2} - \arctan(\sqrt{2 \tan^2 x + 1})}{\sin x \sqrt{\sin^2 x + 1}}. \tag{41}$$

Integrating by parts results in

$$I_2 = 4 \ln\left(\sqrt{2 + \cot^2 \frac{\pi}{2n}} + \cot \frac{\pi}{2n}\right)$$

$$\times \left(\frac{\pi}{2} - \arctan \sqrt{2 \tan^2 \frac{\pi}{2n} + 1}\right)$$

$$- 4 \int_{\frac{\pi}{2n}}^{\frac{\pi}{2}} dx \frac{\ln(\sqrt{2 + \cot^2 x} + \cot x)}{\sqrt{2 + \cot^2 x}}. \tag{42}$$

Using the substitution $z = \tan x$, the resulting integration can finally be written in the form[3]

$$I_2 = \pi \ln n + \pi \ln \frac{4}{\pi} - 2K - \frac{\pi}{2} \ln 2 + O\left(\frac{1}{n^2}\right), \quad (43)$$

where $K \approx 0.916$ is Catalan's constant.

Using Eq. (30), the result for the $(d = 2)$-dimensional lattice is

$$\frac{1}{|b|^2} = \frac{4}{N} \sum_{i=1}^{2} \binom{2}{i} \left(\frac{n}{\pi}\right)^i I_i \quad (44)$$

$$= \frac{2}{\pi} \ln N + \frac{8}{\pi^2}(2 - K) + \frac{2}{\pi} \ln \frac{8}{\pi^2} + O\left(\frac{1}{N}\right). \quad (45)$$

### C. Integration of $I_3$

For the third integral $I_3$, we will only evaluate the asymptotic limit for $n \to \infty$. Starting with

$$I_3 = 4 \int_{\frac{\pi}{2n}}^{\frac{\pi}{2}} dx \int_{\frac{\pi}{2n}}^{\frac{\pi}{2}} dy \int_{\frac{\pi}{2n}}^{\frac{\pi}{2}} dz \frac{1}{\sin^2 x + \sin^2 y + \sin^2 z}, \quad (46)$$

we evidently have $I_3 > 0$ independent of $n$. An upper bound for $I_3$ can be obtained using spherical coordinates, that is,

$$I_3 < 4 \int_{\frac{\pi}{2n}}^{\frac{\pi}{2}\sqrt{3}} dr \int_0^{\frac{\pi}{2}} d\varphi \int_{\frac{\pi}{2}}^{\pi} d\theta \frac{r^2 \sin \theta}{\sin^2 x + \sin^2 y + \sin^2 z}. \quad (47)$$

The integrand is bounded in the whole region of integration and in particular also in the limit $r \to 0$; we thus have $I_3 = O(1)$.

Using numerical integration methods, we obtained

$$\lim_{n \to \infty} I_3 = 15.672 \ldots . \quad (48)$$

Substituting again into Eq. (30), we obtain for the normalization of the $(d = 3)$-dimensional lattice:

$$\frac{1}{|b|^2} = \frac{6}{N} \sum_{i=1}^{3} \binom{3}{i} \left(\frac{n}{\pi}\right)^i I_i \quad (49)$$

$$= \frac{6}{\pi^3} I_3 = \Theta(1). \quad (50)$$

### D. Integrations for $d > 3$

We show in this section that $1/b^2 = O(1)$ for all $d \geqslant 3$; actual numerical values can be obtained by integrating expressions of the form (35) using numerical methods. From this, we can deduce that the search time $T$ indeed scales like $T \sim \sqrt{N}$ for $d \geqslant 3$ as will be shown in Sec. IV.

We will proceed by induction: from (50) it is evident that $1/|b|^2 = O(1)$ holds for $d = 3$. Thus, assuming that $1/|b|^2 = O(1)$ holds for some $d \geqslant 3$, it follows from Eq. (30) and $I_i > 0$, that $I_d = O(1)$.

_____

[3]The following result was obtained using MATHEMATICA.

It remains to be shown that $1/|b|^2 = O(1)$ also holds for $d + 1$. The starting point is again provided by Eq. (30), but this time for $d + 1$, that is,

$$\frac{1}{|b|^2} = 2(d + 1) \left[ \sum_{i=1}^{d} \binom{d + 1}{i} \frac{n^{i-d-1}}{\pi^i} I_i + \frac{1}{\pi^{d+1}} I_{d+1} \right]. \quad (51)$$

The sum of the first $d$ terms adds to a leading order of $1/n$, since $I_i = O(1)$ for $3 \leqslant i \leqslant d$ and the lower-order terms $I_2 = \Theta(\ln N)$ and $I_1 = \Theta(n)$ have prefactors $n^{1-d}$ and $n^{-d}$, respectively. Therefore, these contributions vanish for $n \to \infty$.

It remains to be shown that $I_{d+1} = O(1)$ and this is done using Eq. (35), that is,

$$I_{d+1} = 2^d \int_{\frac{\pi}{2n}}^{\frac{\pi}{2}} dy_1 \cdots \int_{\frac{\pi}{2n}}^{\frac{\pi}{2}} dy_{d+1} \frac{1}{\sum_{l=1}^{d} \sin^2 y_l + \sin^2 y_{d+1}}. \quad (52)$$

As the squared sines are greater than zero, an upper bound is obtained by dropping the last sine term. Now, the $y_{d+1}$ integration is performed, that is,

$$I_{d+1} \leqslant 2^d \left(\frac{\pi}{2} - \frac{\pi}{2n}\right) \int_{\frac{\pi}{2n}}^{\frac{\pi}{2}} dy_1 \cdots \int_{\frac{\pi}{2n}}^{\frac{\pi}{2}} dy_d \frac{1}{\sum_{l=1}^{d} \sin^2 y_l}$$

$$= \left(\pi - \frac{\pi}{n}\right) I_d, \quad (53)$$

and this results in $I_{d+1} = O(1)$. Thus, the normalization constant $b$ is of the order $O(1)$.

The overall result for the normalization constant is to leading order,

$$\frac{1}{b^2} = \begin{cases} \frac{2}{\pi} \ln N + \frac{8}{\pi^2}(2 - K) + \frac{2}{\pi} \ln \frac{8}{\pi^2} & \text{for } d = 2, \\ \frac{6}{\pi^3} I_3 & \text{for } d = 3, \\ O(1) & \text{for } d \geqslant 4, \end{cases} \quad (54)$$

where $K \approx 0.916$ is Catalan's constant and we found $I_3 \approx 15.672$ asymptotically; see (48). In particular, it has been shown that for $i \geqslant 3$, $\lim_{n \to \infty} I_i$ converges. Thus, the leading order contribution to $b$ can be calculated from Eq. (35) by replacing $\frac{\pi}{2n}$ with 0 and using numerical integration methods.

### E. Localization

The normalization parameter $b$ is at the same time a measure for the localization of $|v_1\rangle$ onto the state $|sv\rangle$ and thus on the target vertex $\vec{v}$; see Eq. (18). Hence, the probability that the search will be localized at the target vertex $|v\rangle$ is proportional to

$$|\langle v_1 | sv \rangle|^2 = b^2. \quad (55)$$

(In fact, $b^2$ gives only a lower bound for the localization probability as $|s\rangle$ fixes the coin space state in which the localized state is measured.)

For estimating the overlap of the two-dimensional eigenspace at the avoided crossing with the basis vector pair $|\phi_0\rangle, |v_1\rangle$, we can resort to the results Eqs. (13) and (24). In particular, we found in (13) that the uniform state $|\phi_0\rangle$ is

mapped onto itself and a component in the direction $U_0|sv\rangle$. One finds by straightforward calculation

$$\langle v_1|U_0|sv\rangle = -\frac{2b}{2N}\sum_{\vec{k}\neq 0}\left(\frac{1}{e^{-ig(1)}-e^{i\theta_{\vec{k}}}}+\frac{1}{e^{-ig(1)}-e^{-i\theta_{\vec{k}}}}\right)$$
(56)

$$= -b\left(1-\frac{1}{N}\right).$$
(57)

The overlap of $|v_1\rangle$ with $U_0|sv\rangle$, that is, the localization on the nearest neighbors is thus of the same order as on the target state $|sv\rangle$ itself. To obtain the last equality $e^{ig(1)}=1$ has been used.

We have shown that the vector $|v_1\rangle$ constructed in the preceding section is localized on the target vertex. We have furthermore shown that the vector space spanned by the orthonormal pair of approximate eigenvectors $\{|\phi_0\rangle,|v_1\rangle\}$ has an order $O(1)$ or $O(1\sqrt{\ln N})$ overlap with itself under the unitary map $U_1$.

## IV. QUANTUM SEARCH AT THE AVOIDED CROSSING

The quantum search algorithm corresponds to a rotation in a lower-dimensional subspace spanned by the eigenvectors at the avoided crossing at $\lambda = 1$, $\omega = 0$. The search is initialized in the state $|\phi_0\rangle$ which has an $O(1)$ overlap with the exact eigenstates at the crossing; see (13). We have constructed a second approximate eigenvector at the crossing, namely, $|v_{\lambda=1}\rangle$ in (23), again with an $O(1)$ overlap with the eigenspace at the avoided crossing. We can thus restrict the analysis to studying the avoided crossing in the subspace of $\mathcal{H}$ spanned by the basis vectors $\{|\phi_0\rangle,|v_1\rangle\}$; this subspace is approximately invariant under the quantum walk $U_1$, as shown in Sec. II B; see also [16,20].

### A. The size of the gap at the avoided crossing

In a first step, we project out the two-dimensional submatrix related to the (approximately) invariant subspace, namely, $(U_1^{2\times 2}) = e^{-iH}$, where $H$ is a Hermitian $2\times 2$ matrix. The entries of $H$ can be determined by calculating the matrix elements of $(U_1^{2\times 2})$ explicitly. Using Eqs. (12), (13), and (24), one obtains to leading order,

$$\langle\phi_0|U_1|\phi_0\rangle = 1 - \frac{2}{N},$$
(58)

$$\langle v_1 \mid U_1|v_1\rangle = 1$$
(59)

for the diagonal elements, and

$$\langle\phi_0|U_1|v_1\rangle = \frac{-2b}{\sqrt{N}},$$
(60)

$$\langle v_1|U_1|\phi_0\rangle = \frac{-2}{\sqrt{N}}\langle v_1 \mid U_0|sv\rangle$$
(61)

$$= \frac{2b}{\sqrt{N}}\left(1-\frac{1}{N}\right)$$
(62)

for the off-diagonal entries, where Eq. (57) has been used for the last equality. Identifying the basis vectors $\{|\phi_0\rangle,|v_1\rangle\}$ with $\{|1\rangle,|2\rangle\}$, we obtain to leading order,

$$U_1^{2\times 2} = \begin{pmatrix} 1 & -\epsilon \\ \epsilon & 1 \end{pmatrix} \quad \text{with} \quad \epsilon = \frac{2b}{\sqrt{N}},$$
(63)

which results in a Hamiltonian

$$H = \begin{pmatrix} 0 & -i\epsilon \\ i\epsilon & 0 \end{pmatrix}.$$
(64)

We note that the coupling term $\epsilon$ scales like $1/\sqrt{N}$ and depends on the normalization constant $b$.

Eigenvectors and eigenvalues of $H$ are easily calculated, that is,

$$\begin{array}{ccc}
\text{eigenvector} & & \text{eigenvalue} \\
|u_1\rangle = \frac{1}{\sqrt{2}}\begin{pmatrix} 1 \\ i \end{pmatrix} & & -\epsilon \\
|u_2\rangle = \frac{1}{\sqrt{2}}\begin{pmatrix} 1 \\ -i \end{pmatrix} & & \epsilon
\end{array}$$
(65)

This means, in particular, that the gap at the avoided crossing behaves like

$$\Delta = 2\epsilon = \frac{4b}{\sqrt{N}} + O\left(\frac{1}{N}\right).$$

The time of search is directly related to the gap $\Delta$; the search starts in the vector $|\phi_0\rangle = 1/\sqrt{2}(|u_1\rangle + |u_2\rangle)$ which after successive iterations becomes

$$\left(U_1^{2\times 2}\right)^t|\phi_0\rangle = e^{-iHt}|\phi_0\rangle = e^{-iHt}\frac{1}{\sqrt{2}}(|u_1\rangle+|u_2\rangle)$$
(66)

$$= \frac{1}{\sqrt{2}}(e^{i\epsilon t}|u_1\rangle + e^{-i\epsilon t}|u_2\rangle).$$
(67)

Thus, for a time $T := \frac{\pi}{2\epsilon} = \frac{\pi}{\Delta}$, one has $e^{\pm i\epsilon t} = \pm i$ and

$$\left(U_1^{2\times 2}\right)^t|\phi_0\rangle = \frac{i}{\sqrt{2}}(|u_1\rangle - |u_2\rangle) = -|v_1\rangle,$$
(68)

which is the localized state. Note that the search time $T$ is inversely proportional to the coupling parameter $\epsilon$ in Eq. (64) and thus to the spectral gap at the avoided crossing. The quantum search algorithm succeeds after $O(\sqrt{N}/b)$ steps and thus faster than any classical search.

## V. RESULTS

Putting everything together, we have now identified the search time in leading order as

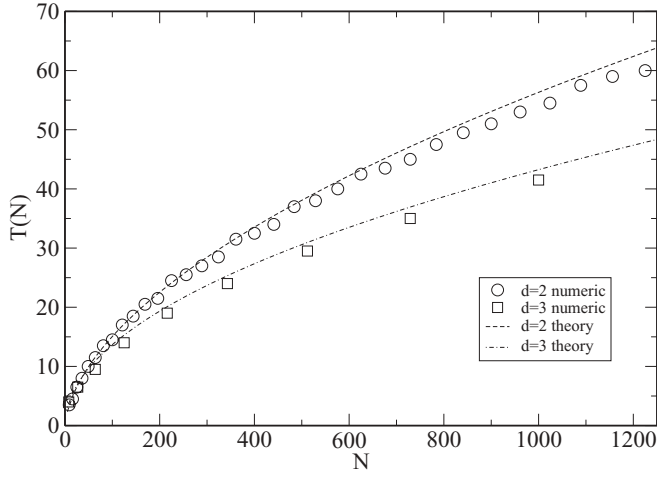$$T = \frac{\pi}{2\epsilon} = \frac{\pi\sqrt{N}}{4b}.$$
(69)

FIG. 3. The localization time $T$ after which the walk is localized at the marked vertex for several $N$. Numerical result compared to analytical for $d = 2$ and 3.

It depends on the normalization constant $b$ which has been obtained in (54). Overall, the number of time steps $T$ can now be given as the integer closest to

$$T = \begin{cases} \frac{\pi\sqrt{N}}{4}\sqrt{\frac{2}{\pi}\ln N + \frac{8}{\pi^2}(2 - K) + \frac{2}{\pi}\ln\frac{8}{\pi^2}} & \text{for } d = 2, \\ \frac{\pi\sqrt{N}}{4}\sqrt{\frac{6I_3}{\pi^3}} & \text{for } d = 3, \\ \Theta(\sqrt{N}) & \text{for } d \geqslant 4. \end{cases}$$

(70)

Note that the bound for $d \geqslant 3$ is tight because we know from [11,19] that the search cannot be faster than $\sqrt{N}$. In Fig. 3, we compare the analytical results for the localization time with numerical simulations. The theoretical results agree very well with the outcome of the numerical simulations. The general behavior suggests that the walk for a fixed number of vertices is the faster the higher the dimension.

The probability to find the search at the target vertex after $T$ steps is equal to $b^2$ (18). From Eq. (54), we find

$$b = \begin{cases} \frac{1}{\sqrt{\frac{2}{\pi}\ln N + \frac{16}{\pi^2} + \frac{4}{\pi}\ln\frac{4}{\pi} - \frac{8K}{\pi^2} - \frac{2}{\pi}\ln 2 + \mathcal{O}(\frac{1}{N})}} = \Theta(\frac{1}{\sqrt{\ln N}}) & \text{for } d = 2, \\ \frac{1}{\sqrt{\frac{6}{\pi^3}I_3}} = \Theta(1) & \text{for } d = 3, \\ \Theta(1) & \text{for } d \geqslant 4. \end{cases}$$

(71)

Note that the upper bound for $b$ in the case $d \geqslant 4$ is a consequence of (69) and the lower bound for the search time is provided by [19].

To leading order, the localization amplitude at the target vertex is not $N$ dependent for $d \geqslant 3$; the $d = 2$ case is exceptional, as the projection of $|v_1\rangle$ onto $|v\rangle$ decreases like $1/\sqrt{\ln N}$. Note, however, that the state $|v_1\rangle$ is still
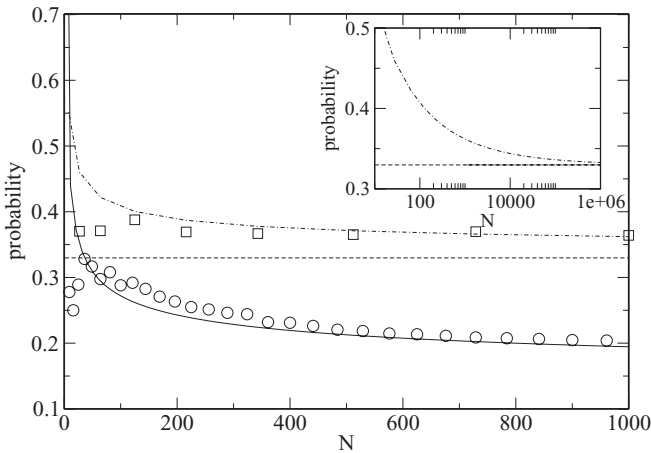


FIG. 4. Maximal probability at the target vertex as a function of $N$. Circles ($d = 2$) and squares ($d = 3$) are obtained directly from the quantum search; the solid and dashed lines represent Eq. (71). The dashed-dotted line gives the result for $b^2$ obtained directly from Eq. (30) for $d = 3$. (Inset) Direct evaluation of Eq. (30) compared with asymptotic result Eq. (71) for $d = 3$ over large $N$ interval.

localized on the marked vertex for $d = 2$ since the average amplitude of an eigenstate of the random walk $U_0$ on an arbitrary vertex decreases like $\frac{1}{\sqrt{N}}$. Amplitude amplification methods can be used to increase the success probability to a constant in $N$ by repeating the search algorithm $O(\sqrt{\ln N})$ times [24].

In Fig. 4, we compare the numerical results for the probability to find the walk at the target vertex with the analytical results for $b^2$. The numerical results are obtained from running the quantum search algorithm and determining the maximum of the probability at the target vertex. It is noted that for $d = 3$, the asymptotic value given in Eq. (71) is not reached before $N \approx 10^6$ (see inset of Fig. 4). This corresponds to a three-dimensional lattice of side length $n = 100$—far beyond what can be simulated on a computer. However, a direct evaluation of $b^2$ in terms of the sums in Eq. (30) confirms the basic mechanism behind our approach.

## VI. CONCLUSIONS

We presented a detailed analysis of the lattice search and show in particular that the search mechanism is based on a rotation from a uniformly extended state to a localized state coupled at an avoided crossing point in the spectrum of the operator $U_\lambda$. The search time and localization strength can be obtained from an effectively two-dimensional model similar to the analysis in [16]. We have thus independently verified the scaling behavior of the search time and localization probability as stated in [15] and can now also give explicit expressions for

the leading order coefficients; the results have been verified by numerical simulations.

A generalization to a search with more than one marked item is straightforward and leads to reduced models as presented in [20]. We also give a detailed derivation of how to obtain the localized state $|\nu_\lambda\rangle$ asymptotically. This is important for the wave communication protocols proposed in [20]; here, the search algorithm is used to search for more than one marked vertex, to send signals through the lattice from a sender to one or more receiver points, and to construct new search algorithms that do not rely on knowing the number of target vertices.

[1] Y. Aharonov, L. Davidovich, and N. Zagury, Phys. Rev. A **48**, 1687 (1993).

[2] J. Kempe, Contemp. Phys. **44**, 307 (2003).

[3] V. Kendon, Phil. Trans. R. Soc. A **364**, 3407 (2006).

[4] M. Santha, in *Proceedings of the 5th International Conference, TAMC 2008, Xi'an, China, April 25–29, 2008*, edited by M. Agrawal, D.-Z. Du, Z. Duan, and A. Li, Lecture Notes in Computer Science (Springer, Berlin, 2008), Vol. 4978, pp. 31–46.

[5] M. Karski, L. Förster, J.-M. Choi, A. Steffen, W. Alt, D. Meschede, and A. Widera, Science **325**, 174 (2009).

[6] H. Schmitz, R. Matjeschk, Ch. Schneider, J. Glueckert, M. Enderlein, T. Huber, and T. Schaetz, Phys. Rev. Lett. **103**, 090504 (2009).

[7] P. Xue, B. C. Sanders, and D. Leibfried, Phys. Rev. Lett. **103**, 183602 (2009).

[8] F. Zähringer, G. Kirchmair, R. Gerritsma, E. Solano, R. Blatt, and C. F. Ross, Phys. Rev. Lett. **104**, 100503 (2010).

[9] H. B. Perets, Y. Lahini, F. Pozzi, M. Sorel, R. Morandotti, and Y. Silberberg, Phys. Rev. Lett. **100**, 170506 (2008).

[10] H. Schreiber, K. N. Cassemiro, V. Potocek, P. J. Mosley, E. Andersson, I. Jex, and Ch. Silberhorn, Phys. Rev. Lett. **104**, 050502 (2010).

[11] L. K. Grover, in *Proceedings of the Twenty-Eighth Annual Symposium on the Theory of Computing, 1996, Philadelphia, Pennsylvania* (ACM Press, New York, 1996), pp. 212–218.

[12] L. K. Grover, Phys. Rev. Lett. **79**, 325 (1997).

[13] N. Shenvi, J. Kempe, and K. B. Whaley, Phys. Rev. A **67**, 052307 (2003).

[14] A. M. Childs and J. Goldstone, Phys. Rev. A **70**, 022314 (2004).

[15] A. Ambainis, J. Kempe, and A. Rivosh, in *Proceedings of the Sixteenth Annual ACM-SIAM Symposium on Discrete Algorithms* (Society for Industrial and Applied Mathematics, Philadelphia, 2005), pp. 1099–1108.

[16] B. Hein and G. Tanner, J. Phys. A **42**, 085303 (2009).

[17] V. Potocek, A. Gabris, T. Kiss, and I. Jex, Phys. Rev. A **79**, 012325 (2009).

[18] A. Tulsi, Phys. Rev. A **78**, 012310 (2008).

[19] C. H. Bennett, E. Bernstein, G. Brassard, and U. Vazirani, SIAM J. Comput. **26**, 1510 (1997).

[20] B. Hein and G. Tanner, Phys. Rev. Lett. **103**, 260501 (2009).

[21] T. Kottos and U. Smilansky, Ann. Phys. **274**, 76 (1999).

[22] S. Gnutzmann and U. Smilansky, Adv. Phys. **55**, 527 (2006).

[23] G. Tanner, in *Non-Linear Dynamics and Fundamental Interactions*, Vol. 213 (Springer, Dordrecht, 2006), p. 69; e-print arXiv:quant-ph/0504224.

[24] L. K. Grover, in *STOC '98: Proceedings of the Thirtieth Annual ACM Symposium on Theory of Computing* (ACM, New York, 1998), pp. 53–62.